

Explaining Monod in Terms of *Escherichia coli* MetabolismEga Danu Chang<sup>1</sup> and Maurice HT Ling<sup>2,3,4\*</sup><sup>1</sup>School of Applied Sciences, Temasek Polytechnic, Singapore<sup>2</sup>Colossus Technologies LLP, Singapore<sup>3</sup>HOHY PTE LTD, Singapore<sup>4</sup>AdvanceSyn Private Limited, Singapore**\*Corresponding Author:** Maurice HT Ling, Colossus Technologies LLP, HOHY PTE LTD, AdvanceSyn Private Limited, Singapore.**Received:** July 29, 2019; **Published:** August 12, 2019**DOI:** 10.31080/ASMI.2019.02.0336**Abstract**

Monod Equation is a simple empirical equation relating limiting substrate to cell growth rate. Despite being used in many studies, there is a need to elucidate growth rate in terms of metabolism, which is then used to inform metabolic engineering efforts. Here, we attempt to explain Monod Equation in terms of simulated metabolism, in the form of metabolic flux, from an *Escherichia coli* MG1655 flux balance analysis (FBA) model to yield a growth rate objective function. Flux values represent change of molecule concentrations over time, making biomass objective function a rate equation. This poses difficulty in representing biomass objective function as a predictive model of metabolic fluxes, which is essentially an analytical equation of fluxes. Our results show a strong correlation ( $r = 0.972$ ,  $p\text{-value} = 1.16 \times 10^{-14}$ ) between Monod's predicted growth rate and biomass objective value from FBA model. Using this relationship, Monod's predicted growth rate can be predicted by 14 fluxes ( $r = 1$ ,  $p\text{-value} < 1 \times 10^{-16}$ ,  $SSE = 2.3 \times 10^{-7}$ ,  $MSE = 1.8 \times 10^{-9}$ ). Therefore, this study explains the growth rate of *E. coli* MG1655 in terms of its metabolic flux and presents a methodology for unifying Monod Equation with simulated or experimental metabolism.

**Keywords:** *Escherichia coli*; Metabolism; Monod Equation**Introduction**

Monod Equation [1] estimates the relationship between limiting carbon source and bacterial growth [2] and is structurally identical to Michaelis-Menten Equation, which models the enzymatic production of product(s) from substrate(s) [3]. Hence, Monod Equation can be seen as an adaptation of Michaelis-Menten Equation for bacterial growth where the substrate and product are carbon source and cellular growth respectively. Recently, Monod Equation has used to model various biological processes, including growth rate [4], product formation kinetics [5], and substrate usage kinetics [6].

The main advantage of using Monod Equation for modelling is its simplicity [7]. Modelling has been shown to be invaluable in metabolic engineering [8], systems biology [9], and synthetic biology [10]. However, Monod Equation, being an empirical formula [11], appears to be inadequate to explain the metabolic processes leading to growth rate. As an empirical relationship, Monod Equation does not render any room for engineering towards industrial objectives; such as increased growth rate or substrate yield rate.

There are recent studies in predicting growth conditions [12] or growth rates in different media [13] from metabolism. However, there has been few attempts to interpret the growth rate in Monod Equation in terms of metabolic rates of various biochemical reactions. Several recent studies have attempted to expand Monod Equation from single substrate to multi-substrate to elucidate metabolism [14-16]. Flux-based models are commonly used in metabolic modeling [17,18]. Although flux models usually include a biomass objective function [19], which corresponds to growth rate; flux values represent change of molecule concentrations over time, making biomass objective function a rate equation and this poses difficulty in representing biomass objective function as a predictive model of metabolic fluxes, which is the presentation of Monod's Equation and is essentially an analytical equation of fluxes. In this study, we attempt to explain Monod Equation in terms of simulated metabolism, in the form of metabolic flux, from an *Escherichia coli* flux balance analysis [20] model to yield a growth rate objective function. This study also presents a methodology for unifying Monod Equation with simulated or experimental metabolism.

## Methods

**Empirical Growth Rate Prediction:** The Monod Equation for *E. coli* growth rate ( $\mu$ ) in divisions per hour in various concentrations of glucose ( $10^{-4}$  M) is given as [2]:  $\mu = \frac{1.35 \times [\text{glucose}]}{2.2 \times 10^{-5} + [\text{glucose}]}$ . Hence, predicted growth rate can be estimated for various concentrations of glucose.

**Simulated metabolism:** Simulated metabolism data was obtained by flux balance analysis (FBA) using Cameo [21] via AdvanceSyn Toolkit (<https://github.com/mauriceling/advancesyntoolkit>) on iAF1260 model [22] from the BiGG database [23], which was used in a previous study [12]. iAF1260 model is a genome scale model (GSM) based on *E. coli* MG1655 [22]. Of the 22 medium components defined, 19 were set to 999,999 mmol per gram dry weight per hour (mmol/gDW/h); representing non-rate limiting quantities. These 19 components are (a) calcium (EX\_ca2\_e), (b) chloride (EX\_cl\_e), (c) carbon dioxide (EX\_co2\_e), (e) cobalt (EX\_cobalt2\_e), (f) copper (EX\_cu2\_e), (g) ferrous (EX\_fe2\_e), (h) ferric (EX\_fe3\_e), (i) water (EX\_h2o\_e), (j) proton (EX\_h\_e), (k) potassium (EX\_k\_e), (l) magnesium (EX\_mg2\_e), (m) manganese (EX\_mn2\_e), (o) molybdate (EX\_mobd\_e), (p) sodium (EX\_na1\_e), (q) ammonium (EX\_nh4\_e), (r) phosphate (EX\_pi\_e), (s) sulfate (EX\_so4\_e), (t) tungstate (EX\_tungs\_e), and (u) zinc (EX\_zn2\_e). Cob(I)alamin (EX\_cbl1\_e) and oxygen (EX\_o2\_e) were set to 0.01 mmol/gDW/h and 18.5 mmol/gDW/h respectively. Simulated metabolic data and its corresponding predicted growth rate, as estimated by the biomass objective function [19], were obtained by varying D-glucose (EX\_glc\_D\_e) concentration which was originally set to 8.0 mmol/gDW/h.

**Determining Growth Rate Objective Function:** Growth rate objective function was determined using stepwise regression using Akaike information criterion [24] from MASS [25] on the following model,  $\mu = \sum_{i=1}^N \beta_i M_i + \beta_0$ ; where  $\mu$  is the growth rate predicted by Monod Equation,  $\beta_i M_i$  are the coefficient and flux (in mmol/gDW/h) of *i*-th molecule obtained from FBA respectively, and  $\beta_0$  is the constant. The flux data from simulation of iAF1260 model was cleaned – all fluxes smaller than 1 nmol/gDW/h were considered zero and variance of fluxes of zero across various glucose uptake rates were removed as they represent constant metabolite concentrations within the cell.

## Results and Discussion

### Estimation of glucose uptake rate required for maximum growth rate

From the Monod Equation given by Liu [2], the growth rate plateau at a maximum of 1.35 divisions per hour. Monk *et al.* [26] ex-

amined the growth rate and the glucose uptake rate of seven strains of *E. coli*, including MG1655 which iAF1260 model [22] was based. Regression analysis (Figure 1) shows that division rate per hour = 0.0591 (glucose uptake rate in mmol/gDW/h) + 0.2465; with significant coefficient of determination ( $R^2$ ) of 0.6877 ( $F = 11.01$ ,  $p$ -value = 0.021). The gradient of 0.0591 is significant ( $t = 3.32$ ,  $p$ -value = 0.02) but the intercept of 0.2465 is not significant ( $t = 1.44$ ,  $p$ -value = 0.21). Using the regression equation, 1.35 divisions per hour will require a glucose uptake rate of 18.67 mmol/gDW/h.

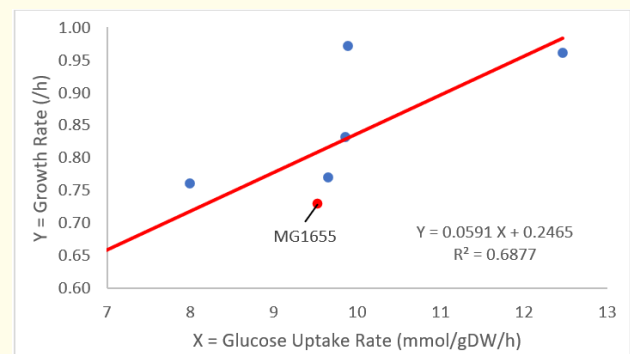


**Figure 1:** Correlation between growth rate and glucose uptake rate in seven strains of *E. coli*. Data point for *E. coli* MG1655 is labeled in red.

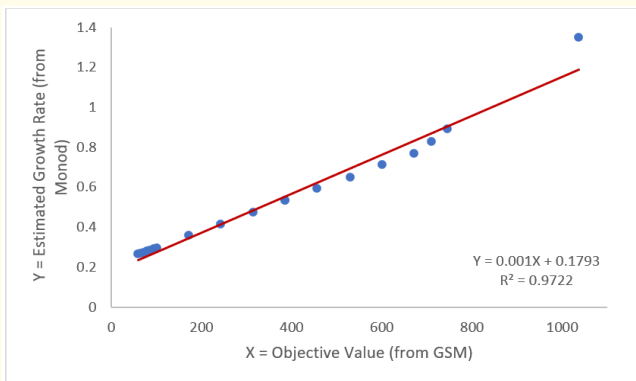
### Strong correlation between biomass objective and growth rate

iAF1260 FBA model is a genome scale model based on *E. coli* MG1655 [22] and its corresponding predicted growth rate in varying D-glucose concentrations can be estimated by the biomass objective function [19]. Our results show a strong correlation ( $r = 0.972$ ,  $p$ -value =  $1.16 \times 10^{-14}$ ) between Monod's predicted growth rate and biomass objective value from FBA model (Figure 2). This suggests a strong possibility to estimate growth rate, in terms of number of cell divisions per hour, from metabolic fluxes, in terms of millimoles per gram dry weight per hour; by using the regression model between growth rate and biomass objective value as proxy.

### No Differences between flux balance analysis and parsimonious flux balance analysis

Cameo [21] provided two means to estimate objective value and fluxes; namely, flux balance analysis (FBA) and parsimonious flux balance analysis (pFBA). The objective values from FBA and pFBA in iAF1260 model [22], analyzed using 1 to 18 mmol/gDW/h of glucose uptake at the interval of 1 mmol/gDW/h ( $n = 18$ ), shows perfect correlation ( $F = 3.17 \times 10^8$ ,  $p$ -value =  $8.29 \times 10^{-60}$ , Figure 3).

(a)



(b)

**Figure 2:** Relationship between biomass objective value and growth rate. Panel A shows the overlay between FBA biomass objective value at various glucose uptake rate and Monod's growth rate at various glucose concentrations. Panel B shows the correlation between biomass objective value from genome scale model (GSM) and growth rate from Monod's Equation.

The regression slope of almost one also suggests that the objective values from FBA and pFBA are similar. A comparison between all 2,382 fluxes from FBA and pFBA in three glucose uptake rates (1, 9, and 18 mmol/gDW/h to represent low, medium and high glucose uptake rates) were analyzed and the correlations between the fluxes from both methods are close to perfect correlation ( $r > 0.999$ ,  $F > 3.84 \times 10^6$ ,  $p\text{-value} < 1 \times 10^{-100}$ ). The regression slopes of fluxes are above 0.9997 and the y-intercepts not significant from zero ( $p\text{-value} > 0.6$ ). These also suggest no differences between FBA and pFBA.

#### Determination of growth rate by flux

The biomass objective function (BiGG ID BIOMASS\_Ec\_iAF1260\_core\_59p81M) in iAF1260 model [19] is defined as a reaction of 63 reactants and 4 products where the objective value, representing

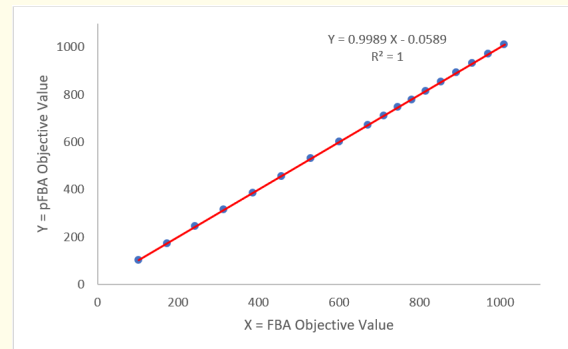


**Figure 3:** Correlation between objective values from FBA and pFBA.

predicted growth rate, is represented as a flux value. Flux values represent the increasing or decreasing concentrations of molecules over time; hence, the biomass objective function is essentially a rate equation. This poses difficulty in representing biomass objective function as a predictive model of metabolic fluxes, which is essentially an analytical equation of fluxes.

130 glucose uptake rates between 0.4 mmol glucose/gDW/h and 18.8 mmol glucose/gDW/h were used to estimate metabolic fluxes, resulting in 309,660 (130 glucose uptake rates  $\times$  2,382 fluxes) data points. From 2,382 metabolic fluxes in iAF1260 model [22], 81.4% ( $n = 1,940$ ) fluxes were constant and removed, resulting in 442 metabolic fluxes remaining. Of the 442 fluxes, the coefficients of 424 fluxes were not defined due to multicollinearity, resulting in 18 fluxes remaining. Of these 18 fluxes, 16 (Figure 4) were found to be significant ( $t\text{-statistic} > 7 \times 10^6$ ,  $p\text{-value} < 2 \times 10^{-16}$ ) by stepwise regression using Akaike information criterion [24] from MASS [25].

**Figure 4:** Correlation as coefficient of determination ( $r^2$ ) between significant fluxes

The regression model between growth rate (divisions per hour) and flux (mmol/gDW/h) is

$$\begin{aligned} \text{Growth rate} = & 0.15390 - \\ & 0.00067 (\text{ACKr flux}) - \\ & 0.00067 (\text{ADK1 flux}) + \\ & 0.00985 (\text{ATPS4rpp flux}) + \\ & 0.01773 (\text{CYTBO3\_4pp flux}) + \\ & 0.01576 (\text{H2Otex flux}) + \\ & 0.00985 (\text{H2Otp flux}) + \\ & 0.00788 (\text{Htex flux}) + \\ & 1.12 \times 10^{-7} (\text{NADTRHD flux}) - \\ & 0.00067 (\text{NDPK1 flux}) + \\ & 0.00017 (\text{NDPK2 flux}) - \\ & 0.01970 (\text{PGK flux}) - \\ & 0.02691 (\text{PGM flux}) + \\ & 0.00067 (\text{PPM flux}) - \\ & 0.02691 (\text{SUCDi flux}) \end{aligned}$$

Where ACKr is acetate kinase, ADK1 is adenylate kinase, ATP-S4rpp is periplasmic ATP synthase, CYTBO3\_4pp is periplasmic cytochrome oxidase bo3 (ubiquinol-8:4 protons), H<sub>2</sub>O tex is extracellular to periplasm water transport via diffusion, H<sub>2</sub>Otp is periplasmic water transport via diffusion, Htex is extracellular to periplasm proton transport via diffusion, NADTRHD is NAD transhydrogenase, NDPK1 is ATP:GDP nucleoside-diphosphate kinase, NDPK2 is ATP:UDP nucleoside-diphosphate kinase, PGK is phosphoglycerate kinase, PGM is phosphoglycerate mutase, PPM is phosphopentomutase, and SUCDi is irreversible succinate dehydrogenase. Regression analysis suggest that Monod's predicted growth rate can be reliably predicted by these 14 fluxes ( $r = 1$ ,  $p$ -value  $< 1 \times 10^{-16}$ ) with negligible error (SSE =  $2.3 \times 10^{-7}$ , MSE =  $1.8 \times 10^{-9}$ ).

Of the 14 fluxes, 3 fluxes (H2Otex, H2Otp, and Htex) are diffusion transport while the remaining 11 fluxes (ACKr, ADK1, ATP-S4rpp, CYTBO3\_4pp, NADTRHD, NDPK1, NDPK2, PGK, PGM, PPM, and SUCDi) are enzymes. Nine of the 11 enzymes; namely, acetate kinase (ACKr) [27]; adenylate kinase (ADK1) [28]; ATP synthesis [29], potentially affected by periplasmic ATP synthase (ATPS4rpp); cytochrome oxidase bo3 [30], potentially periplasmic cytochrome oxidase bo3 (CYTBO3\_4pp); nucleoside-diphosphate kinases [31], potentially NDPK1 and NDPK2; phosphoglycerate kinase (PGK) [32]; phosphoglycerate mutase (PGM) [33]; phosphopentomutase (PPM) [34]; have been shown to affect growth rates of various bacterial strains. NAD transhydrogenase (NADTRHD) has been suggested to affect the growth rate of *E. coli* by affect the fluxes in pentose phosphate pathway [35]. Succinate dehydrogenase has

been shown to affect anaerobic growth of *E. coli* [36] but knocking out irreversible succinate dehydrogenase (SUCDi) has minimal effect on *E. coli* aerobic growth rate but results in massive changes to other metabolites and fluxes [37]. This suggests that the effect of SUCDi on growth rate may be conditional or by modulating other fluxes.

Comparing the regression model and biomass objective function [19] in iAF1260 model [22], the most significant observation is a complete disjoint where none of the fluxes in the regression model are found in the biomass objective function. The biomass objective function consists of 67 metabolites while our regression model consists of 14 transporters and enzymes. Hence, there are two advantages of our regression model. Firstly, our regression model consists of substantially fewer independent variables compared to the biomass objective function. Secondly, metabolite concentrations are at the metabolic level, which cannot be easily manipulated experimentally; unlike enzyme concentrations, which are easier to manipulate using gene over-expression or under-expression. In conclusion, this study explains the growth rate of *E. coli* MG1655 using 2 transport fluxes and 11 enzyme fluxes, as well as presenting a methodology for unifying Monod Equation with simulated or experimental metabolism.

### Conflict of Interest

The authors declare no conflict of interest.

### Bibliography

1. J Monod. "The growth of bacterial cultures". *Annual Review of Microbiology* 3.1 (1949): 371-394.
2. Y Liu. "Overview of some theoretical approaches for derivation of the Monod equation". *Applied Microbiology and Biotechnology* 73.6 (2007): 1241-1250.
3. K A Johnson and R S Goody. "The Original Michaelis Constant: Translation of the 1913 Michaelis-Menten Paper". *Biochemistry* 50.39 (2011): 8264-8269.
4. Á González-Garcinuño A., *et al.* "Effect of bacteria type and sucrose concentration on levan yield and its molecular weight". *Microbial Cell Factories* 16.1 (2017): 91.
5. N A Ramli R., *et al.* "Microbial growth kinetics in isobutanol production by *saccharomyces cerevisiae*". *Chemical Engineering Transactions* 56 (2017): 793-798.
6. L Kopec., *et al.* "The application of Monod equation to denitrification kinetics description in the moving bed biofilm reactor (MBBR)". *International Journal of Environmental Science and Technology* 16.3 (2019): 1479-1486.

7. K Kovárová-Kovar and T Egli. "Growth kinetics of suspended microbial cells: From single-substrate-controlled growth to mixed-substrate kinetics". *Microbiology and Molecular Biology Reviews* 62.3 (1998): 646.
8. O D Kim., *et al.* "A review of dynamic modeling approaches and their application in computational strain optimization for metabolic engineering". *Frontiers in Microbiology* 9 (2018): 1690.
9. Z Ji., *et al.* "Mathematical and computational modeling in complex biological systems". *BioMed Research International* (2017): 1-16.
10. Y Zheng and G Sriram. "Mathematical modeling: Bridging the gap between concept and realization in synthetic biology". *Journal of Biomedicine and Biotechnology* (2010): 1-16.
11. H Hazrati., *et al.* "Biodegradation kinetics and interactions of styrene and ethylbenzene as single and dual substrates for a mixed bacterial culture". *Journal of Environmental Health Science and Engineering* 13 (2015): 72.
12. V Sridhara., *et al.* "Predicting growth conditions from internal metabolic fluxes in an in-silico model of *E. coli*". *PLOS ONE* 9.12 (2014): e114608.
13. R Adadi., *et al.* "Prediction of microbial growth rate versus biomass yield by a metabolic network with kinetic parameters". *PLOS Computational Biology* 8.7 (2012): e1002575.
14. B Shapiro., *et al.* "Integrating genome-scale metabolic models into the prediction of microbial kinetics in natural environments". *Geochimica et Cosmochimica Acta* 242 (2018): 102-122.
15. M Kastelic., *et al.* "Dynamic metabolic network modeling of mammalian Chinese hamster ovary (CHO) cell cultures with continuous phase kinetics transitions". *Biochemical Engineering Journal* 142 (2019): 124-134.
16. F J Barajas-Rodriguez., *et al.* "Simulation of in situ biodegradation of 1,4-dioxane under metabolic and cometabolic conditions". *Journal of Contaminant Hydrology* 223 (2019): 103464.
17. Z Dai and J W Locasale. "Understanding metabolism with flux analysis: From theory to application". *Metabolic Engineering* 43 (2017): 94-102.
18. D Sarkar T., *et al.* "A diurnal flux balance model of *Synechocystis* sp. PCC 6803 metabolism". *PLOS Computational Biology* 15.1 (2019): e1006692.
19. M Feist and B O Palsson. "The biomass objective function". *Current Opinion in Microbiology* 13.3 (2010): 344-349.
20. J D Orth., *et al.* "What is flux balance analysis?". *Nature Biotechnology* 28.3 (2010): 245-248.
21. J G R Cardoso., *et al.* "Cameo: A Python library for computer aided metabolic engineering and optimization of cell factories". *ACS Synthetic Biology* 7.4 (2018): 1163-1166.
22. M Feist., *et al.* "A genome-scale metabolic reconstruction for *Escherichia coli* K-12 MG1655 that accounts for 1260 ORFs and thermodynamic information". *Molecular Systems Biology* 3 (2007): 121.
23. Z A King., *et al.* "BiGG Models: A platform for integrating, standardizing and sharing genome-scale models". *Nucleic Acids Research* 44 (2016): D515-D522.
24. H Akaike. "Information theory and an extension of the maximum likelihood principle". In *Selected Papers of Hirotugu Akaike* (1998): 199-213.
25. B. Ripley., *et al.* "Package 'mass,'" Cran R, 2013.
26. J M Monk., *et al.* "Multi-omics quantification of species variation of *Escherichia coli* links molecular features with strain phenotypes". *Cell Systems* 3.3 (2016): 238-251.
27. B Enjalbert., *et al.* "Acetate fluxes in *Escherichia coli* are determined by the thermodynamic control of the Pta-AckA pathway". *Scientific Reports* 7 (2017): 42135.
28. T T Thach., *et al.* "Adenylate kinase from *Streptococcus pneumoniae* is essential for growth through its catalytic activity". *FEBS Open Bio* 4 (2014): 672-682.
29. N B Shah and T M Duncan. "Aerobic growth of *Escherichia coli* is reduced, and ATP synthesis is selectively inhibited when five C-terminal residues are deleted from the  $\epsilon$  subunit of ATP synthase". *Journal of Biological Chemistry* 290.34 (2015): 21032-21041.
30. J Richhardt., *et al.* "Evidence for a key role of cytochrome bo<sub>3</sub> oxidase in respiratory energy metabolism of *Gluconobacter oxydans*". *Journal of Bacteriology* 195.18 (2013): 4210-4220.
31. M Chakrabarty. "Nucleoside diphosphate kinase: role in bacterial growth, virulence, cell signalling and polysaccharide synthesis". *Molecular Microbiology* 28.5 (1998): 875-882.
32. M M Nakano., *et al.* "A mutation in the 3-phosphoglycerate kinase gene allows anaerobic growth of *Bacillus subtilis* in the absence of ResE kinase". *Journal of Bacteriology* 181.22 (1999): 7087-7097.

33. S Benoit, *et al.* "Treponema pallidum 3-phosphoglycerate mutase is a heat-labile enzyme that may limit the maximum growth temperature for the spirochete". *Journal of Bacteriology* 183.16 (2001): 4702-4708.
34. F Meyer, *et al.* "Methanol-essential growth of *Escherichia coli*". *Nature Communications* 9.1 (2018): 1508.
35. H Zeng and A Yang. "Modelling overflow metabolism in *Escherichia coli* with flux balance analysis incorporating differential proteomic efficiencies of energy pathways". *BMC Systems Biology* 13.1 (2019): 3.
36. E Maklashina, *et al.* "Anaerobic expression of *Escherichia coli* succinate dehydrogenase: functional replacement of fumarate reductase in the respiratory chain during anaerobic growth". *Journal of Bacteriology* 180.22 (1998): 5989-5996.
37. D McCloskey, *et al.* "Growth adaptation of *gnd* and *sdhCB* *Escherichia coli* deletion strains diverge from a similar initial perturbation of the transcriptome". *Frontiers in Microbiology* 9 (2018): 1793.

**Volume 2 Issue 9 September 2019**

**© All rights are reserved by Ega Danu Chang and Maurice HT Ling.**